Asymmetric magnetization reversal in ferromagnetic/antiferromagnetic bilayers

2007 J. Phys.: Condens. Matter 19 236225

(http://iopscience.iop.org/0953-8984/19/23/236225)

IOP PUBLISHING JOURNAL OF PHYSICS: CONDENSED MATTER

J. Phys.: Condens. Matter **19** (2007) 236225 (10pp) doi:10.1088/0953-8984/19/23/236225

Asymmetric magnetization reversal in ferromagnetic/antiferromagnetic bilayers

Jing Chen, Guojun Jin[1] and Yu-qiang Ma

National Laboratory of Solid State Microstructures and Department of Physics, Nanjing University, Nanjing 210093, People's Republic of China

E-mail: gjin@nju.edu.cn

Received 30 January 2007, in final form 27 March 2007
Published 16 May 2007
Online at stacks.iop.org/JPhysCM/19/236225

Abstract
The asymmetric magnetization reversal in exchange-biased ferromagnetic (FM)/antiferromagnetic (AFM) bilayers is studied by the Monte Carlo method. Based on the calculations for both the random and regular configurations of dilution in the AFM layer, it is revealed that the asymmetry is closely related to the domain structure in the AFM layer. The coherent rotation of the magnetization in the FM layer is proven to be the dominant process for the appearance of the asymmetric magnetization reversal. A set of hysteresis loops is obtained for various angles between the external field and the anisotropic direction and for different thicknesses of the FM layer. The numerical results are in good agreement with the recent experimental measurements. In addition, the temperature dependence of the asymmetry is also studied. For a given angle, there is a maximum asymmetry at a certain temperature. Our results indicate that the asymmetry uniquely originates from the unidirectional anisotropy, and its magnitude is determined by the competition between the unidirectional anisotropy and the uniaxial anisotropy.

1. Introduction

For a coupled bilayer composed of a ferromagnetic (FM) layer and an antiferromagnetic (AFM) layer, due to the existence of interfacial exchange couplings, some interesting properties have appeared. The most important effect is the shift of its hysteresis loop along an external magnetic field H from $H = 0$ when the whole system is cooled below the Néel temperature T_N of the AFM layer. This phenomenon is known as the exchange bias, and has attracted intense attention because of its wide applications in high-density magnetic recording media and spin valve devices. Though it was discovered by Meiklejohn and Bean [1] more than 50 years ago, there has been no satisfactory understanding yet of the microscopic mechanism of the effect.

[1] Author to whom any correspondence should be addressed.

Recently, an important problem in exchange-biased systems is the explanation of the asymmetry in the magnetization reversal. The reversal asymmetry of a hysteresis loop was first discovered in Fe/FeF_2 [2], then it was also observed in other exchange-biased systems. Some researchers have interpreted it as different magnetization mechanisms for each branch of the hysteresis loop. For example, it was reported that the coherent rotation of the magnetization is the main mechanism for the descending branch of the loop, whereas for the ascending branch the mechanism changes to the domain wall nucleation and propagation [2, 3]. The opposite possibility was also suggested, that the coherent magnetization rotation takes place on the ascending branch of the loop, but domain walls nucleate on the descending branch [4–7]. The origin of the asymmetric reversal is still a debated issue. The FM anisotropy in high order may be responsible for the origin of the asymmetric reversal [8–10]. Within the framework of the domain state model, Beckmann *et al* [11] proposed that the angle between the external field and the FM or AFM easy axis strongly affects the asymmetry of the magnetization reversal, and different angles result in different reversal processes, e.g., a coherent rotation on both branches of a hysteresis loop or a nonuniform reversal on the ascending branch. Some other researchers considered the training effect [12, 13]. In a recently published paper, based on the excellent experimental results and the modified Stoner–Wohlfarth model, Camarero *et al* [14] suggested that the asymmetric magnetization reversal strongly depends on the competition between the unidirectional anisotropy caused by the interface coupling and the uniaxial anisotropy of the FM layer.

The exchange bias is an interfacial effect. However, the lack of detailed knowledge of the interface makes the problem very complicated. So far, a systematic study of the asymmetric magnetization reversal is still absent, especially concerning the role of the AFM layer, such as its microstructures, anisotropy, and temperature dependence. Under this situation, numerical study provides a useful tool for solving the problem. In this paper, the Monte Carlo method is adopted to investigate the mechanism behind the magnetization reversal asymmetry from a microscopic point of view. Comparing with the preceding work by Beckmann *et al* [11], we further consider the magnetization reversal asymmetry from different domain structures of the AFM layer, the thickness variation of the FM layer, and especially the effect of temperature.

The paper is organized as follows: section 2 is about the model and method. Presented in section 3 are the simulation results for the dependence of asymmetry on the thickness of the FM layer and the temperature, as well as a reasonable interpretation for the reversed mechanism. Finally, a summary is given in section 4.

2. Model and method

It is well known that the domain state model [15] has been used successfully to explain some aspects relating to the exchange bias, such as the thickness dependence, the temperature dependence and the training effect. However, there are some discrepancies in the asymmetry reversal between the simulation results based on the domain state model [11] and the experimental results [14]. This may be caused by the difference of the domain structures in the AFM layer between the simulations and the experiments. Therefore, in order to interpret the experimental results, the domain state model needs to be improved by considering the possible distribution of nonmagnetic sites in the AFM layer for the simulations. Concretely, we consider an IrMn alloy system here. It is interesting to note that the strength of the Ir–Mn or Ir–Ir bonds is weaker than that of the Mn–Mn bonds [16]. Therefore, the Ir–Mn and Ir–Ir bonds in the system are assumed to be in a broken state and these broken bonds can be replaced by the nonmagnetic defects. There are two possibilities for distributing the nonmagnetic defects in the AFM layer; one is random and the other is regular. The simulation results will show the difference between the random distribution and the regular distribution.

The system consists of N_{FM} FM monolayers and N_{AFM} AFM monolayers, where N_{FM} and N_{AFM} are positive integers. Nonmagnetic defects are distributed randomly or regularly in the AFM layer. In our calculations, we choose the concentration of nonmagnetic sites $p = 0.25$ for both the random and regular dilutions. In the case of the random dilution, nonmagnetic sites are distributed randomly in the two sublattices. But in the case of the regular dilution, there are many ways to distribute nonmagnetic sites. A simple and possible structure is used here. In each AFM monolayer, the sites of one sublattice are fully occupied by the magnetic atoms, and the sites of the other sublattice are occupied by the magnetic and nonmagnetic atoms alternately. For two neighbouring monolayers, the nonmagnetic atoms are located in different sublattices. For such a geometric arrangement, the magnetization of the whole AFM layer is zero and provides a partial compensated interface.

In order to obtain the possible domain structures in the AFM layer, a large enough system must be taken. Here we adopt the rather large lattice size 128×128 in the layer plane for the random distribution, while for the regular distribution the lattice size 64×64 is enough. The layer plane is denoted by the y and z coordinates. The periodic boundary conditions are applied to the y and z directions and the free boundary condition in the x direction. To investigate the spin structure and the magnetization process of this bilayer system, the classical Heisenberg model is used for a simple cubic lattice. The exchange interactions of the AFM layer are considered up to the next-nearest neighbours. Because of the broken nearest-neighbouring bonds, the interactions between the next-nearest neighbours play a role to stabilize the long-range order. It is observed in our simulations that the asymmetry is decreased a little when there are no next-nearest-neighbouring interactions.

The model Hamiltonian is

$$\mathcal{H} = \mathcal{H}_{\mathrm{FM}} + \mathcal{H}_{\mathrm{AFM}} + \mathcal{H}_{\mathrm{INT}}, \tag{1}$$

where $\mathcal{H}_{\mathrm{FM}}$, $\mathcal{H}_{\mathrm{AFM}}$, and $\mathcal{H}_{\mathrm{INT}}$ describe the spin configurations of the FM layer, AFM layer and the interface coupling between the FM and AFM layers, respectively. They are

$$\mathcal{H}_{\mathrm{FM}} = -J_{\mathrm{FM}} \sum_{\langle i,j \rangle} \boldsymbol{S}_i \cdot \boldsymbol{S}_j - \sum_i (d_z S_{iz}^2 + d_x S_{ix}^2 + \boldsymbol{S}_i \cdot \boldsymbol{H}), \tag{2}$$

$$\mathcal{H}_{\mathrm{AFM}} = -J_1 \sum_{\langle i,j \rangle} \epsilon_i \epsilon_j \sigma_i \cdot \sigma_j - J_2 \sum_{\langle i,k \rangle} \epsilon_i \epsilon_k \sigma_i \cdot \sigma_k - \sum_i \epsilon_i (k_z \sigma_{iz}^2 + \sigma_i \cdot \boldsymbol{H}), \tag{3}$$

and

$$\mathcal{H}_{\mathrm{INT}} = -J_{\mathrm{INT}} \sum_{\langle i,j \rangle} \epsilon_j \boldsymbol{S}_i \cdot \sigma_j, \tag{4}$$

where $\boldsymbol{S}_i$ and $\boldsymbol{\sigma}_i$ represent spins at the ith site of the FM and AFM layers, respectively. The first term in equation (2) is the exchange interaction in the FM layer with the exchange constant J_{FM}. The other part in the bracket of equation (2) is the contribution from the uniaxial anisotropy and the Zeeman energy caused by an external field. We take the z-axis as its easy axis with an anisotropy constant d_z and the x-axis as its hard axis with a shape anisotropy constant d_x. The first two terms in equation (3) are the exchange interaction of the AFM layer with the nearest-neighbouring exchange constant J_1 and the next-nearest-neighbouring exchange constant J_2. $\epsilon_i = 0$ (1) represents a nonmagnetic (magnetic) site. The third term in equation (3) is the uniaxial anisotropy with the z-axis as its easy axis, where k_z is the anisotropy constant. The fourth term is the Zeeman energy of the AFM layer. Equation (4) is the interaction energy at the interface of the FM and the AFM layer with the exchange constant J_{INT}.

For the simple cubic lattice and the parameters chosen, the simulation results give the reduced Curie temperature $T_{\mathrm{C}} = 2.9$ and Néel temperature $T_{\mathrm{N}} = 1.5$, where the temperatures are scaled by $J_{\mathrm{FM}}/k_{\mathrm{B}}$. To reproduce the experimental measurements of a field-cooled system,

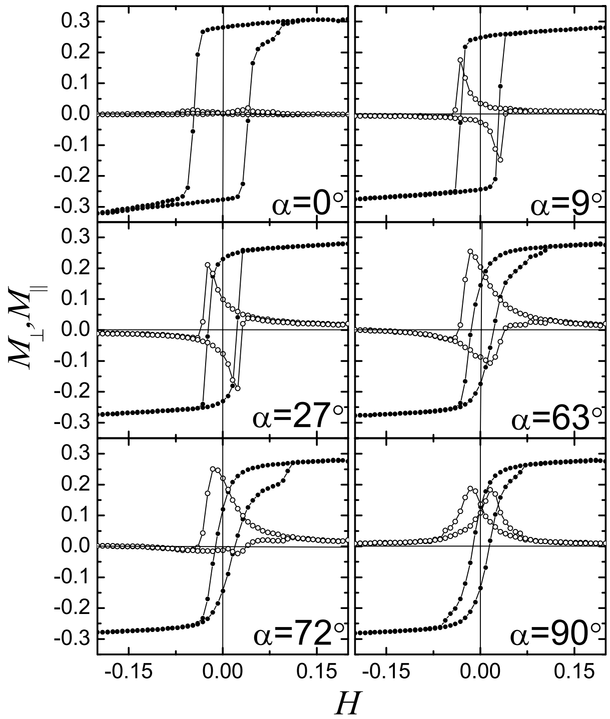

Figure 1. Hysteresis loops of the magnetizations $M_\parallel$ (solid circles) and $M_\perp$ (open circles) versus external field at different angles α in the case of randomly distributed nonmagnetic sites with $N_{AFM} = 3$ and $N_{FM} = 1$.

we start from a random configuration at the temperature $T = 2.6$, which is between T_C and T_N, and follow the quasicontinuous cooling process down to the measurement temperatures of the system with the magnetic field $H_{CF} = 0.3J_{FM}$ and a constant temperature step $\Delta T = -0.05$. We employ the Monte Carlo method [17] with single-spin flips and the heat bath algorithm. During the simulations, the parameters used are $J_{INT} = J_{FM}/2$, $J_1 = -J_{FM}/2$, $J_2 = |J_1|/2$, $d_z = 0.05J_{FM}$, $d_x = -0.2J_{FM}$, and $k_z = J_{FM}$. The hysteresis loops for the magnetizations parallel and perpendicular to external fields are measured by starting from $H = 0.2J_{FM}$ down to $-0.2J_{FM}$ and then rising again up to the initial value with a constant step $\Delta H = 0.008J_{FM}$. For a complete hysteresis loop we perform typically 40 000 Monte Carlo steps and the results are averaged by repeating the runs for five different random numbers.

3. Results and discussion

Because an asymmetric magnetization can only be observed when the external field is not collinear with the easy axis of the AFM layer or the cooling field, it is essential to study the angle dependence of the asymmetry. Figures 1 and 2 give the simulation results of the $M_\parallel$ and $M_\perp$ hysteresis loops under the random and regular distributions of nonmagnetic sites. $M_\parallel$ and $M_\perp$ represent the magnetizations parallel and perpendicular to the external field, respectively. Both the $M_\parallel$ and $M_\perp$ loops exhibit the pronounced asymmetry. In figure 1, it is clear that the exchange bias and coercivity of the $M_\parallel$ loops decrease with increasing angle α. More interestingly, the descending and ascending branches of the $M_\perp$ loops evolve from two different

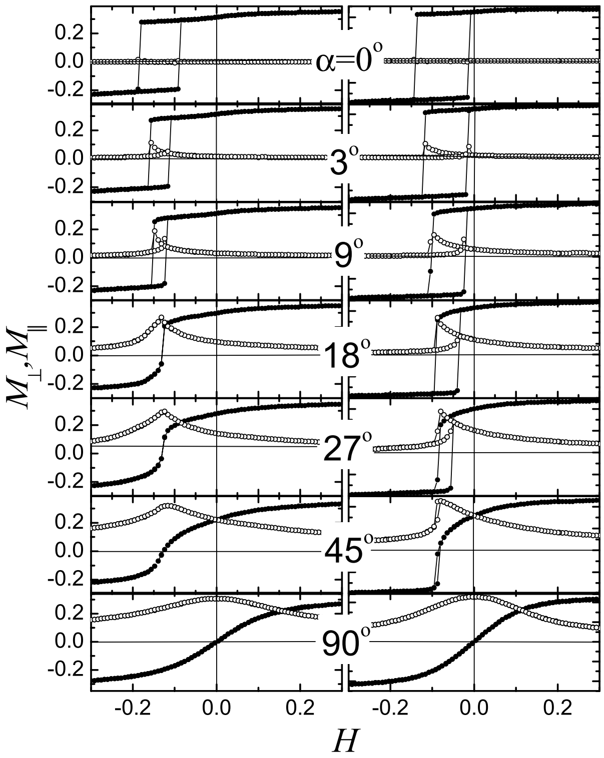

Figure 2. Hysteresis loops of the magnetizations $M_\parallel$ (solid circles) and $M_\perp$ (open circles) at different angles in the case of regularly distributed nonmagnetic sites with the same AFM thickness, $N_{\rm AFM} = 3$, but two different FM thicknesses, $N_{\rm FM} = 1$ (left column) and 2 (right column).

directions to the same direction at a certain angle. Moreover, even when the external field is perpendicular to the unidirectional anisotropy, the coercivity can still be observed, which is consistent with the experiments [18, 19]. Compared to the results of Beckmann *et al* [11], we observe a maximum asymmetric reversal at 72°, while their results show a maximum asymmetric reversal at 60°. The reason is that there is a smaller exchange bias at $p = 0.25$ than $p = 0.6$. From our simulations, it is found that the different concentrations of nonmagnetic sites lead to different domain structures and the asymmetry is strongly influenced by the change of the AFM domain structures. From the simulation results shown in figure 2, an important fact is that a larger exchange bias occurs in the regular distribution than in the random distribution. This is comparable in order of magnitude to the experimental results [14]. Correspondingly, the evolution of the $M_\perp$ hysteresis loop is only along the same direction, and the magnetization rotates reversibly with increasing the angle. By comparing figure 1 with 2, it is obvious that the characteristics of magnetizations are strongly influenced by different AFM domain structures. The simulation results indicate that the random distribution is in good agreement with the previous simulations [11], while the regular distribution is closer to the existing experiments [14]. To judge this statement, it could be suggested to perform new experiments on samples with precisely random distribution of nonmagnetic sites.

In order to further study the relationship between reversal mechanism and domain structure, we analyse the different reversal mechanisms of the random and regular distributions at first. We choose the angle at which the maximum asymmetry appears, where 72° is for the

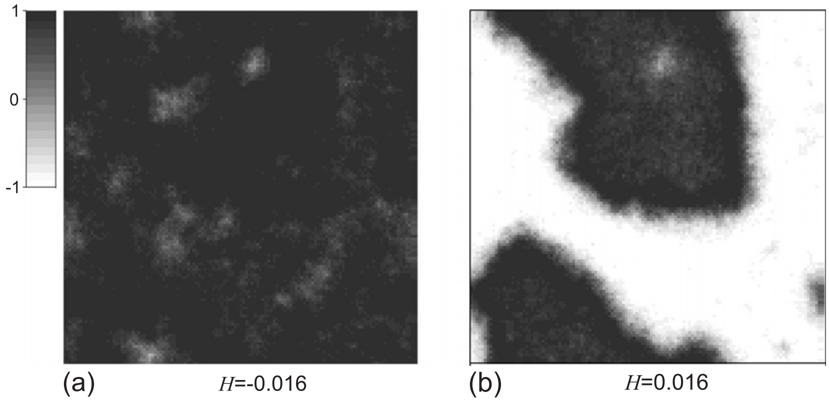

Figure 3. Two snapshots of the FM spin configurations at the FM/AFM interface at 72° for the random distribution of nonmagnetic sites, corresponding to the descending (a) and ascending (b) branches of the magnetization loop, respectively.

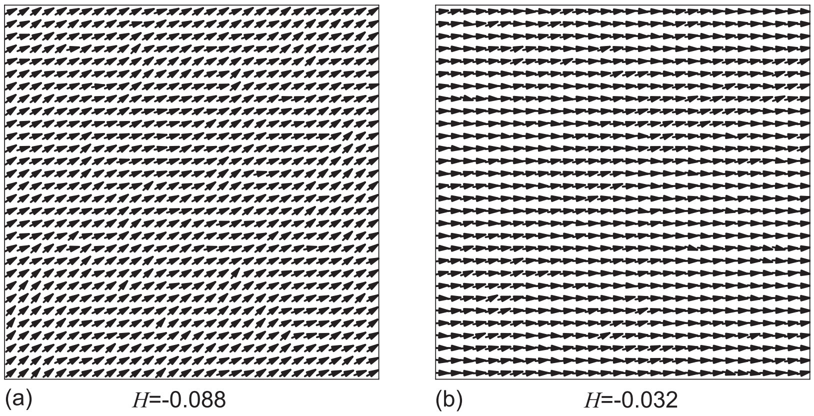

Figure 4. Two snapshots of the FM spin configurations at the FM/AFM interface at 18° for the regular distribution of nonmagnetic sites, corresponding to the descending (a) and ascending (b) branches of the magnetization loop, respectively.

random distribution and 18° for the regular distribution. Figures 3 and 4 give the FM spin configurations at the FM/AFM interface for two different angles. Two snapshots of the spin configurations correspond to two peaks of $M_{\perp}$, respectively. From figure 3, it can be seen that the reversal process is mainly the coherent rotation at the descending branch, while at the ascending branch a nearly 180° FM domain wall is formed as shown in figure 3(b), which indicates that the reversal mechanism is mainly the domain wall nucleation and propagation. For the regular distribution, both branches verify the coherent rotation, as shown in figure 4.

The different reversal mechanisms may be caused by the different domain structures of the random and regular distributions. It is known that domain walls are always easy to form on the nonmagnetic sites. For the random distribution, the AFM layer is frozen into a domain state. This domain structure results in an inhomogeneous pinning on the FM layer. Due to the unidirectional nature of the AFM pinning field, on the ascending branch the field causing the reversal of the FM layer comes from the competition between the inhomogeneous interfacial pinning and the uniaxial anisotropy, which leads to the domain wall nucleation and propagation,

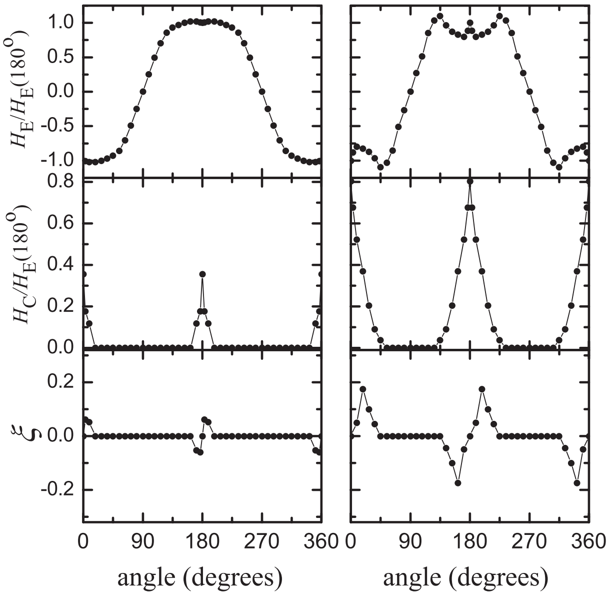

Figure 5. Simulated exchange bias, coercivity, and asymmetry versus angle for the same parameters as in figure 2: the same AFM thickness, $N_{AFM} = 3$, and two different FM thicknesses, $N_{FM} = 1$ (left column) and 2 (right column).

while on the descending branch they are in the same direction, strengthening the FM rotation. It is clear that the main mechanism is the coherent rotation. For the regular dilution, domain walls are distributed uniformly on average. A homogeneous pinning on the FM layer is provided by the AFM domain. Thus, the reversal process of the FM layer is the coherent rotation. Here, it becomes obvious that the distributions of the nonmagnetic sites will change the spin microstructures of the AFM layer, which give rise to different domain structures and different reversal processes, but they are not relevant for the appearance of the asymmetry. It could be trusted that the coherent rotation is the main reversal process.

A parameter ξ is used to denote the angle and thickness dependence of the asymmetry [14], and is defined by the gap between the absolute values of two peaks of an $M_\perp$ loop. Figure 5 systematically shows the angle and thickness dependence of exchange bias, coercivity, and asymmetry. It can be found that the asymmetry effect is restricted in the range of some angles. Above a certain angle, only the reversible transition is shown, and the asymmetry disappears. This angle is named the critical angle. With increasing FM thickness, the critical angle increases, as shown in figure 5 for $N_{FM} = 1$ and 2. In fact, when the thickness increases, the ratio of the uniaxial anisotropy and unidirectional anisotropy increases. Therefore, the asymmetry and the critical angle also increase. This shows the same tendency as in the experimental measurements [14], except a smaller magnitude. The reason for a smaller magnitude can be almost recognized as the difference between the simulated systems and the realistic systems, such as various system parameters and material structures.

The temperature dependence of the reversal asymmetry is very important, since the magnetic devices are always operated in surroundings of variable temperatures [20]. However, there have seldom been theories considering the temperature dependence till now. The Monte Carlo method provides a good approach to study this problem. Figure 6 shows the $M_\parallel$ and $M_\perp$ hysteresis loops simulated at different temperatures. From the $M_\parallel$ hysteresis loops, it is obvious that the exchange bias decreases monotonically, while the coercivity increases first and then decreases with increasing temperature. As for $M_\perp$, it reverses only along one direction in the low-temperature range; with further increase of the temperature the directions of the two

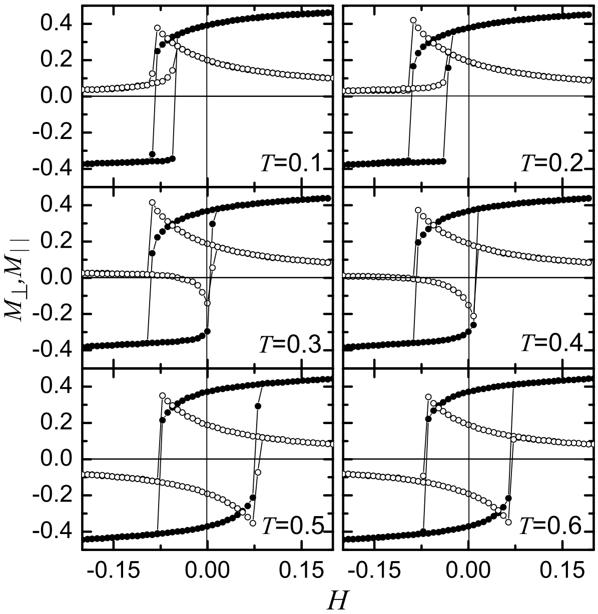

Figure 6. Hysteresis loops of the magnetization $M_\parallel$ (solid circles) and $M_\perp$ (open circles) at different temperatures. The angle between the external field and FM easy axis is 27°.

branches become opposite. This temperature effect can be interpreted by the model adopted by Beckmann *et al* [11]. The field applied to the FM layer comprises three parts, namely, the anisotropic field along the easy axis of the FM layer ($H_A = 2d_z m_{z\mathrm{FM}}$), the exchange field of the AFM layer along the bias direction ($H_X = J_{\mathrm{INT}} m_{z\mathrm{AFM}}$), and the external field (H). The three fields are superposed to form a total effective field influencing the magnetization process. The anisotropic field depends on the projection of the reduced FM magnetization $m_{z\mathrm{FM}}$, and points in two different directions on either branch of a hysteresis loop. The exchange field is determined by the z-component of the reduced AFM magnetization $m_{z\mathrm{AFM}}$. It is reasonable to assume that $m_{z\mathrm{AFM}}$ decreases with increasing temperature more quickly than $m_{z\mathrm{FM}}$ does. At low temperatures, the magnitude of the exchange field is larger than that of the anisotropic field. The component of the effective field perpendicular to the external field points to the same direction on both branches. Therefore, $M_\perp$ reverses only in one direction. Once the magnitude of the exchange field is smaller than that of the anisotropic field at high temperatures, the component points in two different directions, and then $M_\perp$ reverses along the opposite directions.

The simulation results for the behaviour of the bias field, coercivity and asymmetry varied with temperature are presented in figure 7 at two different angles. The exchange bias decreases slowly with increasing temperature. At a certain temperature, which is generally called the block temperature, the exchange bias drops to zero. The coercivity increases gradually with increasing temperature, and a peak appears near the block temperature; after this the coercivity decreases until reaching a stable value. These simulation results are in good agreement with the experimental measurements for the FeF_2/Fe bilayer [21] and theoretical results [22]. A simple analysis can be given as that at low temperatures, the AFM layer is nearly ordered, the FM magnetization drags fewer AFM spins, thus the pinning of the AFM layer only contributes to the exchange bias, while the coercivity approaches the value of the free FM layer; as the temperature increases, the FM magnetization is able to drag more and more AFM spins, enhancing the coercivity; above the block temperature, the AFM layer is random and does not affect the FM rotation, then the coercivity reduces. It can be seen that the asymmetry increases at low temperatures but decreases at high temperatures and there is a peak below the block

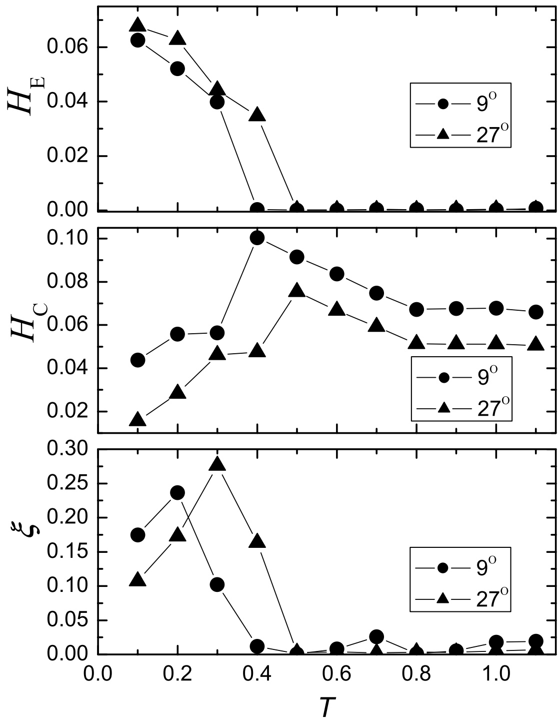

Figure 7. Simulated exchange bias, coercivity, and asymmetry versus temperature at the angles 9° (circle) and 27° (triangle).

temperature. At the block temperature, the asymmetry disappears. It can be interpreted as before by the superposition of the three fields, namely H_A, H_X, and H. As the temperature increases, H_X and H_A decrease. When $H_A = H_X$, the effective field perpendicular to the external field is $H_X - H_A = 0$. Thus, $M_{\perp \mathrm{right}}$ takes the minimum value and ξ reaches the maximum value. It is obvious that the competition between the unidirectional anisotropy and the uniaxial anisotropy causes the change of the asymmetry. This result is consistent with the theoretical calculations [10]. In fact, the asymmetry disappears at the block temperature, which confirms our consideration that the asymmetry, just like the exchange bias, originates from the unidirectional anisotropy.

4. Summary

We have studied the asymmetric magnetization reversal in ferromagnetic/antiferromagnetic bilayers by the Monte Carlo method in a multifaceted way. Firstly, we have investigated the influence of domain structures in the AFM layer on the asymmetry. In contrast to the previous simulations, the different concentrations of defects have been adopted to display the size effect of domains. Our simulation results demonstrate that the defects in the AFM layer favour domain formation and the domain structures are crucial for the existence of the unidirectional anisotropy. In this case the reversal asymmetry is solely determined by the unidirectional anisotropy because the uniaxial anisotropy is fixed in the FM layer. Secondly, by using two different configurations for dilution in the AFM layer, the mechanism for the asymmetry has been clarified. It is proven that the change of the AFM domain structures causes different reversal mechanisms, especially the coherent rotation or the domain wall nucleation and propagation. But the emergence of asymmetry is not relevant to the domain wall nucleation and propagation. The coherent rotation is still the unique mechanism for the asymmetry. Thirdly, for the different FM thicknesses, we have systematically investigated the relation between the asymmetric magnetization reversal and the angle of the external field with the FM anisotropic direction. We have confirmed that with increasing uniaxial anisotropy both the critical angle and asymmetry increase. Finally, we have investigated the temperature effect on the asymmetry. When the exchange bias diminishes with increasing temperature, the asymmetry disappears accordingly. This simultaneous tendency implies that the asymmetry is the essential character of exchange bias systems. The simulation results also show that there is a peak during the increase of the temperature, which is caused by the competition between the unidirectional anisotropy and the uniaxial anisotropy. According to the theoretical results obtained, we can conclude that by tuning the FM and AFM anisotropies, the temperature, the exchange coupling, and the angle of the external field with the anisotropic direction, it is hopeful to control the magnitudes of the coercivity, the exchange bias and the asymmetry for designing magnetic devices.

Acknowledgments

This work was supported by the Natural Science Foundation 60371013, 10674058, the Provincial Natural Science Foundation of Jiangsu BK2002086, and the State Key Program for Basic Research of China 2006CB921803.

References

[1] Meiklejohn W H and Bean C P 1956 *Phys. Rev.* **102** 1413
Meiklejohn W H and Bean C P 1957 *Phys. Rev.* **105** 904
[2] Fitzsimmons M R, Yashar P, Leighton C, Schuller I K, Nogués J, Majkrzak C F and Dura J A 2000 *Phys. Rev. Lett.* **84** 3986
[3] Leighton C, Fitzsimmons M R, Yashar P, Hoffmann A, Nogués J, Dura J, Majkrzak C F and Schuller I K 2001 *Phys. Rev. Lett.* **86** 4394
[4] Radu F, Etzkorn M, Schmitte T, Siebrecht R, Schreyer A, Westerholt K and Zabel H 2002 *J. Magn. Magn. Mater.* **240** 251
[5] Gierlings M, Prandolini M J, Fritzsche H, Gruyters M and Riegel D 2002 *Phys. Rev.* B **65** 092407
[6] Liu Z Y and Adenwalla S 2003 *Phys. Rev.* B **67** 184423
[7] Eisenmenger J, Li Z P, Macedo W A A and Schuller I K 2005 *Phys. Rev. Lett.* **94** 057203
[8] Mewes T, Nembach H, Rickart M, Demokritov S O, Fassbender J and Hillebrands B 2002 *Phys. Rev.* B **65** 224423
[9] Krivorotov I N, Leighton C, Nogués J, Schuller I K and Dahlberg E D 2002 *Phys. Rev.* B **65** 100402
[10] Tillmanns A, Oertker S, Beschoten B, Güntherodt G, Eisenmenger J and Schuller I K 2005 *Preprint* cond-mat/0509419
[11] Beckmann B, Nowak U and Usadel K D 2003 *Phys. Rev. Lett.* **91** 187201
[12] Dorfbauer F, Suess D, McCord J, Kirschner M, Schrefl T and Fidler J 2005 *J. Magn. Magn. Mater.* **290/291** 754
[13] Hoffmann A 2004 *Phys. Rev. Lett.* **93** 097203
[14] Camarero J, Sort J, Hoffmann A, García-Martín J M, Dieny B, Miranda R and Nogués J 2005 *Phys. Rev. Lett.* **95** 057204
[15] Miltényi P, Gierlings M, Keller J, Beschoten B, Güntherodt G, Nowak U and Usadel K D 2000 *Phys. Rev. Lett.* **84** 4224
[16] Ali M, Marrows C H, Al-Jawad M, Hickey B J, Misra A, Nowak U and Usadel K D 2003 *Phys. Rev.* B **68** 214420
[17] Landau D P and Binder K 2000 *A Guide to Monte Carlo Simulations in Statistical Physics* (Cambridge: Cambridge University Press)
[18] Hoffmann A, Grimsditch M and Pearson J E 2003 *Phys. Rev.* B **67** 220406
[19] Chung S H, Hoffmann A and Grimsditch M 2005 *Phys. Rev.* B **71** 214430
[20] Hu J G, Jin G and Ma Y Q 2004 *Eur. Phys. J.* B **40** 265
[21] Shi H, Liu Z and Lederman D 2005 *Phys. Rev.* B **72** 224417
[22] Scholten G, Usadel K D and Nowak U 2005 *Phys. Rev.* B **71** 064413